Magnetic field and orientation dependence of solid-state CIDNP

Denis V. Sosnovsky,[1,2] Nikita N. Lukzen,[1,2] Hans-Martin Vieth,[1,3] Gunnar Jeschke,[4]

Daniel Gräsing,[5] Pavlo Bielytskyi,[5] Jörg Matysik,[5] Konstantin L. Ivanov*[1,2]

[1] *International Tomography Center, Siberian Branch of the Russian Academy of Science, Novosibirsk, 630090, Russia*

[2] *Novosibirsk State University, Novosibirsk, 630090, Russia*

[3] *Freie Universität Berlin, Institute of Experimental Physics, 14195 Berlin, Germany*

[4] *ETH Zürich, Department of Chemistry and Applied Biosciences, 8093 Zürich, Switzerland*

[5] *Universität Leipzig, Institut für Analytische Chemie, 04103 Leipzig, Germany*

Abstract

The magnetic field dependence of Chemically Induced Dynamic Nuclear Polarization (CIDNP) in solid-state systems is analyzed theoretically with the aim to explain the puzzling sign change of polarization found at low fields [Sci. Rep., 7 (2017) 12111]. We exploit the analysis of polarization in terms of level crossings and level anti-crossings trying to identify the positions of features in the CIDNP field dependence with specific crossings between spin energy levels of the radical pair. Theoretical treatment of solid-state CIDNP reveals a strong orientation dependence of polarization due to the spin dynamics conditioned by anisotropic spin interactions. Specifically, different anisotropic CIDNP mechanisms become active at different magnetic fields and different molecular orientations. Consequently, the field dependence and orientation dependence of polarization need to be analyzed together in order to rationalize experimental observations. By considering both magnetic field and orientation dependence of CIDNP, we are able to explain the previously measured CIDNP field dependence in photosynthetic reaction centers and to obtain a good qualitative agreement between experimental observations and theoretical results.

* Corresponding author, e-mail: ivanov@tomo.nsc.ru

I. Introduction

Chemically Induced Dynamic Nuclear Polarization (CIDNP) is a hyperpolarization technique that can be applied for NMR signal enhancement and for studies of short-lived radical species. CIDNP is formed in diamagnetic products of chemical reactions having radical pair (RP) intermediates[1]. Such photo-induced RP reactions (H-transfer) have been observed by Stehlik et al.[2-4] in monocrystalline matrices doped with dye molecules. They proceed via a triplet precursor followed by spin-selective decay back to the singlet ground state and lead to efficient nuclear polarization mainly in avoided crossing regions. While CIDNP in liquids is based on mechanisms which are well understood, solid-state CIDNP[5] represents a more complex case due to the presence of non-averaged anisotropies of spin interactions. Analysis of solid-state CIDNP is also complicated because of the limited number of chemical systems, in which solid-state CIDNP effects have been reported, and by technical difficulties in running solid-state CIDNP experiments. Presently, the molecular systems that exhibit solid-state CIDNP effects are limited to photosynthetic reactions centers[6-10] and flavoproteins[11]. As far as the interpretation of solid-state CIDNP is concerned, it usually considers a number of mechanisms, termed differential relaxation (DR), differential decay (DD) and three-spin mixing (TSM). Our recent paper[12] shows that one can look at CIDNP from a more general perspective of level crossing phenomena by associating the features in the field dependence to specific Level Crossings (LCs) and Level Anti-Crossings (LACs). By using this kind of description, we were able to obtain analytically positions of the features in the CIDNP field dependences and to derive the sign rules for polarization.

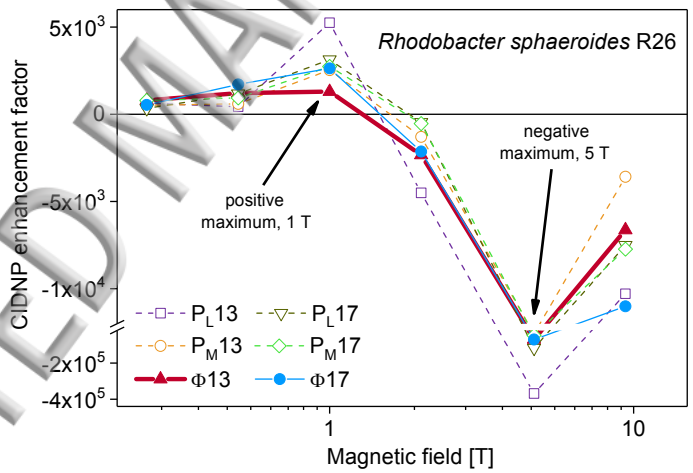

Figure 1. Experimental CIDNP field dependence obtained for the photosynthetic reaction center of the purple bacterium *Rhodobacter sphaeroides* R26. The field dependence of the **C13Φ** nucleus is highlighted. See text for further explanation.

Recent experimental studies of the CIDNP field dependence in solids[13] show that polarization exhibits a rather unexpected behavior, see **Figure 1**: while at high field the observed CIDNP can be explained by the TSM concept, at low field CIDNP changes its sign. This puzzling observation stimulated us to revisit the theoretical treatment of CIDNP and to reveal what the relative contributions are from the individual mechanisms at different magnetic fields. Hence, in this work we study the field dependence of CIDNP. Since the relevant anisotropic interactions strongly depend on the molecular orientation, we also study the orientation dependence of polarization. As we demonstrate below, both dependences of CIDNP are strongly interrelated in the sense that

This manuscript was accepted by J. Chem. Phys. Click here to see the version of record.

specific orientations give rise to maxima of polarization at very different field strengths. For this reason, we analyze the CIDNP field dependence for different orientations. We also correlate the orientation dependence of polarization at different fields with the orientation dependence of relevant anisotropic interactions in order to elucidate their role in the polarization formation. Such an analysis allows us to rationalize the magnetic field dependence of solid-state CIDNP and to make comparison with experimental findings.

The outline of the paper is as follows. In Section II, we describe the theoretical model and briefly explain the known CIDNP mechanisms in the solid-state, as well as additional mechanisms that we have found when analyzing the CIDNP orientation and field dependence. In Section III, we present numerical results for the orientation and field dependence of polarization, showing that both dependences need to be analyzed together.

II. Theory

A. Theoretical model

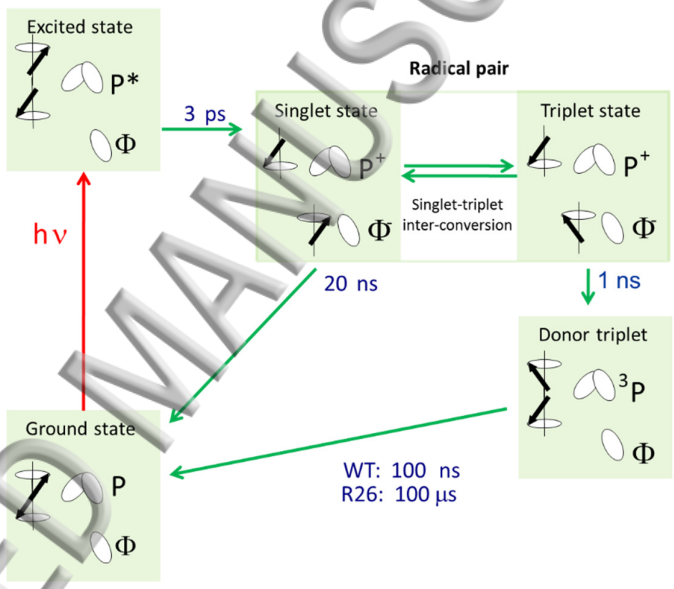

Scheme 1. Photocycle of quinone-depleted or quinone-reduced photosynthetic reaction centers of *Rhodobacter* (*R.*) *sphaeroides* wildtype (WT) and the carotenoidless mutant R26. In R26, the triplet lifetime τ_T is about 100 µs, whereas triplet transfer to a carotenoid reduces it to about 100 ns in mutant R26. **P** refers to the primary electron donor, a dimer of two bacteriochlorophyll molecules, and **Φ**, a pheophytin cofactor, to the electron acceptor. The spin-correlated radical pair is formed by radicals of **P** and **Φ**.

In this work, we consider CIDNP formed in the reaction cycle shown in **Scheme 1**. This scheme is, in fact, almost identical with the photo-cycle in the paper by Wegner et al.[14], which is an intermediate case between liquid and solid systems insofar as the distance and mutual orientation of dye and quencher is rigid, while molecular tumbling leads to partial averaging of anisotropic interaction: this case is thus bridging the gap between liquid and solid CIDNP. Hence, we assume that the RP is singlet-born, and it can undergo electron back transfer from both the electronic singlet and triplet state, giving rise to the singlet-state reaction product (ground state of the system) and triplet-state reaction product, respectively. The triplet product goes to the singlet ground state

This manuscript was accepted by J. Chem. Phys. Click here to see the version of record.

with a characteristic time τ_T. The evolution of the RP is described by the following equation for its density matrix, ρ:

$$\frac{d}{dt}\rho = -i[\hat{\mathcal{H}}, \rho] - \frac{k_S}{2}\{\hat{\mathcal{P}}_S, \rho\} - \frac{k_T}{2}\{\hat{\mathcal{P}}_T, \rho\} - k_{sc}\rho \quad (1)$$

Here $\hat{\mathcal{H}}$ is the RP spin Hamiltonian, k_S and k_T are the recombination rates of the singlet and triplet RPs, respectively; $\hat{\mathcal{P}}_{S,T}$ are the projectors onto these spin states; k_{sc} is the decay rate of the RP due to spin-independent processes (scavenging, here we set $k_{sc} = 0$ in most cases). Note that Eq. (1) does not preserve the trace of the density matrix ρ, which is intended, since ρ corresponds to only the RP subspace that is depleted by electron back transfer. In principle, it is possible to introduce the density matrix of the reacting system with $\mathrm{Tr}\{\rho\} = 1 = const$ by spanning the basis on the RP states and product states and using Lindblad-type equations.[15] However, in the present case this is an unnecessary complication, since RP recombination is a simple irreversible process. The form of the terms describing the chemical reactions has been discussed in previous publications[16-18]. To introduce the initial condition here we always assume singlet-state RP preparation:

$$\rho(t = 0) = \rho_0 = \frac{1}{4}\hat{E} - (\hat{\mathbf{S}}_1 \cdot \hat{\mathbf{S}}_2) \quad (2)$$

with $\hat{E}$ being the unity operator. For simplicity, in our calculations we always consider an RP with a single magnetic nucleus, which belongs to radical 1. The Hamiltonian of the RP in the external magnetic field $\mathbf{B}_0 || Z$ is of the form (in $\hbar$ units):

$$\hat{\mathcal{H}} = \mu_B \mathbf{B}_0 \hat{\mathbf{g}}_1 \hat{\mathbf{S}}_1 + \mu_B \mathbf{B}_0 \hat{\mathbf{g}}_2 \hat{\mathbf{S}}_2 - \omega_N \hat{I}_z + \hat{\mathbf{S}}_1 \hat{\mathbf{d}} \hat{\mathbf{S}}_2 + \hat{\mathbf{S}}_1 \hat{\mathbf{A}} \hat{\mathbf{I}} \quad (3)$$

Here $\hat{\mathbf{g}}_1$ and $\hat{\mathbf{g}}_2$ are the electronic g-tensors of radical 1 and radical 2, μ_B is the Bohr magneton; $\omega_N = g_N \mu_N B_0 = \gamma_N B_0$ is the nuclear Zeeman interaction. The electron-electron coupling $\hat{\mathbf{d}}$ is given by the contributions of the exchange interaction J_{ex} and the dipole-dipole interaction described by the tensor $\hat{\mathbf{D}}$:

$$\hat{\mathbf{S}}_1 \hat{\mathbf{d}} \hat{\mathbf{S}}_2 = -J_{ex}\left[2(\hat{\mathbf{S}}_1 \cdot \hat{\mathbf{S}}_2) + \frac{1}{2}\right] + \hat{\mathbf{S}}_1 \hat{\mathbf{D}} \hat{\mathbf{S}}_2 \quad (4)$$

Finally, the electron-nuclear hyperfine coupling (HFC) is described by the hyperfine tensor $\hat{\mathbf{A}}$, which takes into account isotropic (contact HFC) as well as anisotropic (dipolar HFC) coupling. Hereafter, we consider only the high-field regime with respect to the electron spin, meaning that the electron Zeeman interactions are much greater than the electron-electron coupling and HFC terms, and we assume small g-anisotropy. This is a valid assumption because for the system under consideration the electron-electron coupling and HFC do not exceed several mT, whereas we consider CIDNP formed at magnetic fields above 100 mT. Likewise, g-anisotropy is small, being of the order of 10^{-3}. Hence, it is sufficient to consider only the zz-component of the g-tensors, secular and non-secular terms in the electron-electron coupling, and also secular and pseudo-secular hyperfine terms. The pseudo-secular hyperfine term is required since the high-field approximation is violated for the nuclear spin. As a consequence, we recast the RP Hamiltonian as follows[12, 19-21]:

This manuscript was accepted by J. Chem. Phys. Click here to see the version of record.

$$\hat{\mathcal{H}} \approx \omega_{1e}\hat{S}_{1z} + \omega_{2e}\hat{S}_{2z} - \omega_N\hat{I}_z + d\left(\hat{S}_{1+}\hat{S}_{2-} + \hat{S}_{1-}\hat{S}_{2+}\right) + a\hat{S}_{1z}\hat{I}_z + b\hat{S}_{1z}\hat{I}_x \quad (5)$$

Hence, the electron Zeeman interactions are written as $\omega_{1e} = g_{zz}^{(1)}\mu_B B_0$ and $\omega_{2e} = g_{zz}^{(2)}\mu_B B_0$; here we also introduce the non-secular part of the electron-electron coupling as $d = -2J_{ex} - D$ where D is the dipolar interaction strength; a is the secular HFC and b is the pseudo-secular HFC. In the following, we will also use the parameters $\Delta g = g_{zz}^{(1)} - g_{zz}^{(2)}$ (difference in the electronic g-factors) and $\Delta\omega_e = \omega_{1e} - \omega_{2e} = \Delta g \cdot \mu_B \cdot B_0$ (difference in the electronic Zeeman interactions with the $\mathbf{B}_0$ field).

In this work, we calculate CIDNP of both singlet and triplet product in the following way[12]:

$$P_S = \mathrm{Tr}\left\{\hat{I}_z \cdot k_\mathrm{S}\int_0^\infty \hat{\mathcal{P}}_\mathrm{S}\rho(t)dt\right\}, \quad P_T = \mathrm{Tr}\left\{\hat{I}_z \cdot k_\mathrm{T}\int_0^\infty \hat{\mathcal{P}}_\mathrm{T}\rho(t)dt\right\} \quad (6)$$

Here the rate of polarization formation from both channels is given by the expressions $k_\mathrm{S}\hat{\mathcal{P}}_\mathrm{S}\rho(t)$ and $k_\mathrm{T}\hat{\mathcal{P}}_\mathrm{T}\rho(t)$; these quantities are multiplied by the $\hat{I}_z$ operator to obtain the expectation value of polarization and integrated from zero to infinity. Finally, we calculate the total CIDNP as a sum of two contributions:

$$P = P_\mathrm{S} + \xi P_\mathrm{T}, \quad \xi = \exp[-\tau_\mathrm{T}/T_1] \quad (7)$$

Here, we multiply P_T by a factor $0 \leq \xi \leq 1$, which takes into account paramagnetically enhanced nuclear T_1-relaxation in the triplet state, which has a lifetime of τ_T. The importance of this step is discussed below.

For evaluating P_S and P_T we propose the following method. First, we rewrite eq. (1) in the Liouville space where ρ is a column-vector:

$$\frac{d}{dt}\rho = i\hat{\hat{\mathcal{H}}}\rho - \hat{\hat{\mathcal{R}}}\rho - k_\mathrm{sc}\rho \quad (8)$$

Accordingly, all terms on the right-hand side are rewritten by introducing super-operators, i.e., matrices in the Liouville space, denoted by double hats. The super-operators describing dynamic evolution and RP recombination are written as follows:

$$\hat{\hat{\mathcal{H}}} = \hat{E} \otimes \hat{\mathcal{H}} - \hat{\mathcal{H}} \otimes \hat{E}, \quad (9)$$

$$\hat{\hat{\mathcal{R}}} = \frac{k_\mathrm{S}}{2}\{\hat{E} \otimes \hat{\mathcal{P}}_\mathrm{S} + \hat{\mathcal{P}}_\mathrm{S} \otimes \hat{E}\} + \frac{k_\mathrm{T}}{2}\{\hat{E} \otimes \hat{\mathcal{P}}_\mathrm{T} + \hat{\mathcal{P}}_\mathrm{T} \otimes \hat{E}\}$$

Here $\otimes$ stands for the direct (Kronecker) product of matrices. Eq. (8) is now easy to solve:

$$\rho(t) = \exp\left[\left(i\hat{\hat{\mathcal{H}}} - \hat{\hat{\mathcal{R}}}\right)t - k_\mathrm{sc}t\right]\rho_0 \quad (10)$$

The expressions for P_S and P_T take the form:

$$P_S = \mathrm{Tr}\left\{\hat{I}_z \cdot k_S\hat{\mathcal{P}}_\mathrm{S}\left[\left(i\hat{\hat{\mathcal{H}}} - \hat{\hat{\mathcal{R}}}\right) - k_\mathrm{sc}\hat{\hat{E}}\right]^{-1}\rho_0\right\} \quad (11)$$

This manuscript was accepted by J. Chem. Phys. Click here to see the version of record.

$$P_T = \mathrm{Tr}\left\{\hat{I}_z \cdot k_T \hat{\mathcal{P}}_\mathrm{T}\left[\left(i\hat{\hat{\mathcal{H}}} - \hat{\hat{\mathcal{R}}}\right) - k_{\mathrm{sc}}\hat{\hat{E}}\right]^{-1}\rho_0\right\}$$

Hence, the problem of calculating CIDNP is reduced to a matrix algebra problem requiring only inversion of super-matrices. One should note that transition to the Liouville space requires dealing with matrices of higher dimensionality. Nonetheless, operations with super-matrices are straightforward, and highly optimized algorithms exist for computing matrix exponentials and for matrix inversion, so that the method proposed turns out to be more numerically efficient than the one we used earlier[12].

B. CIDNP mechanisms

Before presenting the results, let us briefly explain the solid-state CIDNP mechanisms discussed so far and a new mechanism introduced in this work. In principle, one can look at the individual mechanisms from a more general perspective by identifying different mechanisms with particular LCs and LACs in the RPs, which give rise to specific spin mixing and result in features in the CIDNP field dependence. Each LC or LAC then corresponds to particular matching conditions for different terms in the Hamiltonian $\hat{\mathcal{H}}$.

First of all, we need to discuss the main mechanism operative in the case of liquid-state CIDNP at high fields, corresponding to nuclear "spin-sorting" by the chemical reaction. When talking about spin-sorting one must differentiate between nuclear spin sub-ensembles, giving rise to different rates of singlet-triplet interconversion. Since the chemical reactivity depends on the interconversion frequency, it is different for different nuclear spin states, i.e., the chemical reaction "sorts" the nuclear spin states. However, this mechanism does not work when the radical centers do not separate so that all RPs eventually recombine or undergo electron back transfer independent of their nuclear spin state. To make spin sorting operative and to generate steady-state (not transient) CIDNP via this mechanism, a nuclear spin flip is necessary. In solids, spin sorting becomes efficient when RPs can recombine through both singlet and triplet channels and when the triplet polarization relaxes so that $\xi < 1$. In this case, cancellation of CIDNP accumulated in the singlet and triplet product is incomplete and the spin-sorting mechanism comes into play. This scenario gives rise to solid-state CIDNP, although the RP spin dynamics is essentially due to isotropic interactions (isotropic spin mixing comes into play). In solid-state CIDNP literature this mechanism[6] is termed DR (differential relaxation). The sign rule for polarization in this case is as follows:

$$\Gamma = \mathrm{sgn}(\Delta g) \times \mathrm{sgn}(a) \times \mu \times \psi \qquad (12)$$

where $\mu = +1$ for the triplet-born RP and $\mu = -1$ for the singlet-born RP; $\psi = +1$ for polarization in the singlet channel and $\psi = -1$ for polarization in the triplet channel. Nuclear spin relaxation is expected to be faster in the triplet channel due to paramagnetic relaxation enhancement. Hence, the sign of net polarization is expected to be the one for the singlet channel. Maximal polarization is expected when the LC condition is fulfilled, so that $|\Delta g \mu_B B_0| = |a|/2$. When this condition is fulfilled, the interconversion rate in one of the nuclear subensembles becomes zero and spin sorting is most efficient.

A different situation arises when anisotropic interactions come into play. The simplest case is met when the electron-electron interaction is zero. In this case, spin levels $|\alpha\beta\alpha_N\rangle$ and $|\alpha\beta\beta_N\rangle$ have

This manuscript was accepted by J. Chem. Phys. Click here to see the version of record.

an LC (depending on the sign of Δg and A this LC may be found alternatively for the $|\beta\alpha\alpha_N\rangle$ and $|\beta\alpha\beta_N\rangle$ levels). In this case, the pseudo-secular HFC becomes operative and mixes the states so that the LC turns into a LAC. The matching condition is as follows: $|\omega_N| = |a|/2$. Spin mixing at the LAC can give rise to observable CIDNP when the rates k_S and k_T are different;[7] for this reason this mechanism is termed DD (differential decay). The sign rule for the DD mechanism takes the form:

$$\Gamma = \mathrm{sgn}(\Delta g) \times \mathrm{sgn}(a) \times \mu \times \epsilon \tag{13}$$

where $\epsilon = +1$ for $k_S > k_T$ and $\epsilon = -1$ for $k_S < k_T$.

A more complex situation arises when the electron-electron coupling comes into play; this case is usually termed TSM (three-spin mixing)[20]. Detailed analysis shows that the TSM case splits into a bunch of cases depending on the values of different interactions. The original formulation of TSM requires triple matching, i.e., $|\Delta\omega_e| \approx |\omega_N| \approx |a|/2$. While the second condition can be fulfilled at a properly chosen magnetic field strength, the first condition requires a particular value of Δg, which can be achieved for specific molecular orientation when the g-tensors of the radicals are anisotropic. In addition, TSM is operative when Δg is small and when $|\omega_N|$ matches the value of $|d|$. In both cases, the sign rule for CIDNP is the same:

$$\Gamma = -\mathrm{sgn}(d) \times \mathrm{sgn}(g_N) \times \mu \tag{14}$$

TSM requires that anisotropic HFC is present, namely that $b \neq 0$, but it does not impose any requirements on the chemical reactivity. In the TSM case, CIDNP is formed via polarization transfer from electron spins to the nuclei in the RP; hence, the reaction of electron back transfer is needed only to transfer the nuclear polarization to a diamagnetic product.

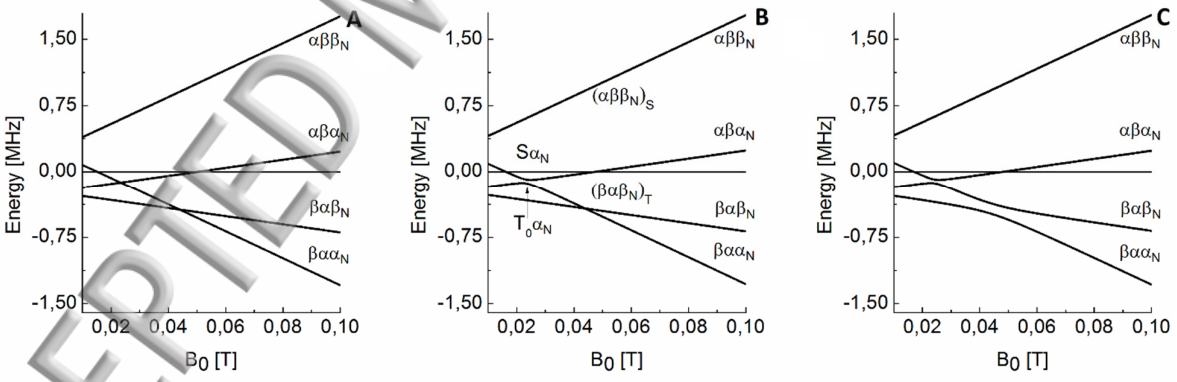

Figure 2. Energy levels of an RP with a single magnetic spin-½ nucleus; here only the electronic states $\alpha\beta$ and $\beta\alpha$ are shown (high-field approximation is used). (A) Electron-electron coupling and pseudo-secular HFC term are neglected; (B) electron-electron coupling is taken into consideration so that the first LC turns into an LAC; (C) pseudo-secular HFC is also taken into account and both LCs turn into LACs. Simulation parameters: $g_A = 2.0035$, $g_D = 2.002$, nucleus is a ^{13}C nucleus, $a = -0.03$ mT, $d = -0.002$ mT (middle and right), $b = 0.012$ mT (right).

Previously, TSM was considered in situations where $|\Delta\omega_e| \leq |\omega_N|$. In this work, we also consider the opposite case $|\Delta\omega_e| > |\omega_N|$ and find a different behavior of the LACs and CIDNP field dependence. Since such a case has not been analyzed before, we discuss it here in detail assuming that $d \neq 0$ and $|\Delta\omega_e| > |\omega_N|$. In the absence of perturbation terms (electron-electron coupling and pseudo-secular HFC) at high magnetic fields, namely in the field range where $\omega_N \leq a$ there are

two LCs (see **Figure 2A**): (i) an LC of the states $|\alpha\beta\alpha_N\rangle$ and $|\beta\alpha\alpha_N\rangle$ occurring when $|\Delta\omega_e| = |\frac{a}{2}|$ and (ii) an LC of the states $|\beta\alpha\beta_N\rangle$ and $|\beta\alpha\alpha_N\rangle$ occurring when$|\omega_N| = |\frac{a}{2}|$. When $|\Delta\omega_e| > |\omega_N|$ the first LC occurs at a lower field (the order of the LCs is inverted as compared to the previously case $|\Delta\omega_e| < |\omega_N|$). As we show below, such an inversion of the energy levels leads to a bimodal structure of the CIDNP magnetic-field dependence having a positive and a negative lobe, see **Figure 3**. To account for the CIDNP effects we take into account the perturbation terms and analyze what the perturbed energy levels and the spin dynamics are. Once the electron-electron coupling comes into play, the first LC turns into an LAC. In the LAC region the eigen-states are modified: the lower state becomes $|T_0\alpha_N\rangle$ and the upper state becomes $|S\alpha_N\rangle$ (if we assume $d < 0$), see **Figure 2B**. At this LAC, no polarization is formed unless pseudo-secular HFC comes into play.

CIDNP formation at the first LC, occurring when $|\Delta\omega_e| = |\frac{a}{2}|$ can be explained in the same way as polarization formation in the TSM case[12, 20, 21], when $d \neq 0$, $|\Delta\omega_e| = |\omega_N|$. For explanation one should note that all four states are involved in the RP spin evolution. The reason is that the electron-electron coupling also mixes the states $|\beta\alpha\beta_N\rangle$ and $|\alpha\beta\beta_N\rangle$: the lower level $|\beta\alpha\beta_N\rangle$ acquires predominantly triplet character (hence, we denote it as $|(\beta\alpha\beta_N)_T\rangle$), while the upper level acquires predominantly singlet character (it is denoted as $|(\alpha\beta\beta_N)_S\rangle$). Due to RP preparation in the singlet state the population of these levels are $\left(\frac{1}{4} - \delta\right)$ and $\left(\frac{1}{4} + \delta\right)$, respectively, where $0 < \delta < \frac{1}{4}$. At the first LAC, the pseudo-secular HFC term mixes three levels, $|T_0\alpha_N\rangle$,$|S\alpha_N\rangle$ and $|(\beta\alpha\beta_N)_T\rangle$, having populations equal to 0, $\frac{1}{2}$ and $\left(\frac{1}{4} - \delta\right)$. After spin mixing, the populations of these states are re-distributed. As a consequence, the β_N nuclear states get overpopulated, hence the nuclear spins acquire negative polarization. Since the type of spin mixing for the first LAC is the same as for the previously described TSM case (i.e., for the case $d \neq 0$, $|\Delta\omega_e| = |\omega_N|$), the sign rule is given by Eq. (14).

At the second LAC occurring when ω_N is matched to the HFC term, see **Figure 2C**, polarization is formed by mixing of the $|T_0\alpha_N\rangle$ and $|(\beta\alpha\beta_N)_T\rangle$ states via the pseudo-secular HFC term. As the $|(\beta\alpha\beta_N)_T\rangle$ state has higher population, spin mixing gives rise to nuclear spin flips $\beta_N \rightarrow \alpha_N$, hence, to positive CIDNP. As a consequence, the CIDNP field dependence has a positive and a negative feature, as shown in **Figure 3**. Such a behavior is general: the sign of polarization for the two LACs is always opposite.

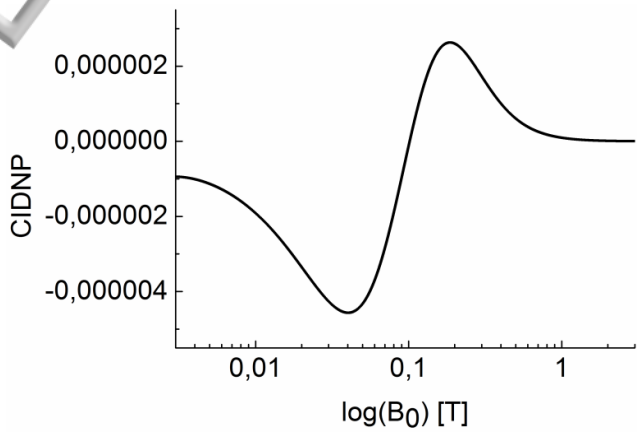

Figure 3. CIDNP field dependence in the case $|\Delta\omega_e| > |\omega_N|$. Simulation parameters: $g_A = 2.0035$, $g_D = 2.002$, nucleus is a ^{13}C nucleus, $a = -0.03$ mT, $d = -0.002$ mT, $b = 0.01$ mT; $k_S = k_T = 0.015$ ns^{-1}, $\xi = 1$.

This manuscript was accepted by J. Chem. Phys. Click here to see the version of record.

The outlined mechanism of CIDNP formation has not been reported before and can be considered as a new solid-state CIDNP mechanism. However, we find it more appropriate to stay with the general description of CIDNP in terms of different LCs/LACs rather than introduce new mechanisms. Hence, we prefer to discuss LCs/LACs and their positions for different sets of parameters.

C. CIDNP in reaction centers, calculation parameters

To perform calculations, we used parameters known experimentally[22-26] for the RC of *Rhodobacter sphaeroides* or derived by DFT computations[27]. The structure of the bacteriopheophytin that acts as an electron acceptor is shown in Scheme 2.

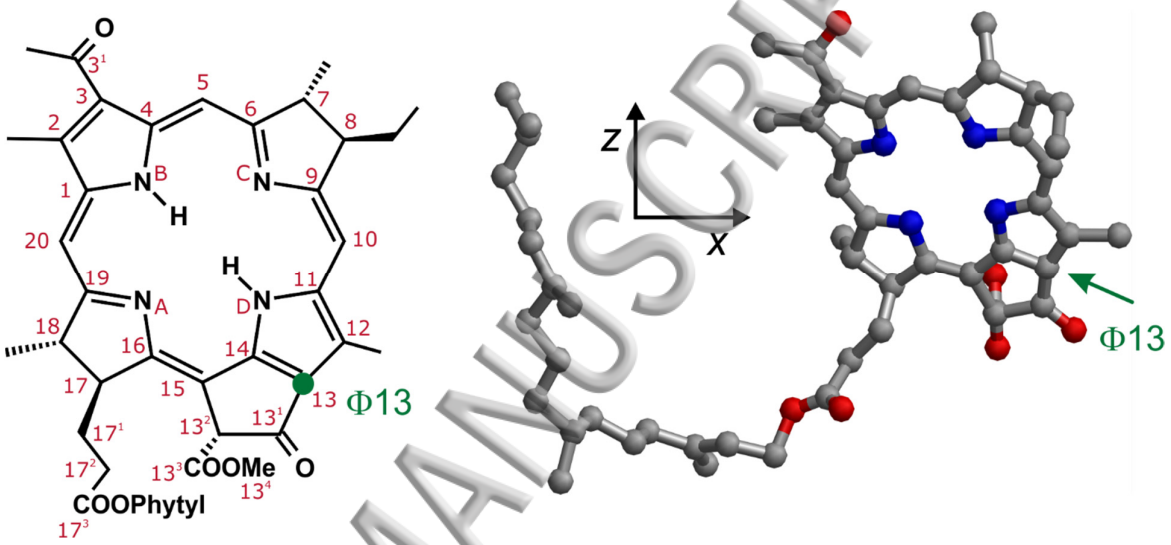

Scheme 2. Structure of the bacteriopheophytin acceptor of the photosynthetic reaction center of the purple bacterium *Rhodobacter sphaeroides* R26. Carbon numbering is given by IUPAC nomenclature. Orientation dependence of the ^{13}C nuclear polarization of nucleus **C13Φ** is considered. The molecular frame (right panel, viewed along the $-y$ direction) is defined by PDB file 1AIJ, where the acceptor is a prosthetic group embedded in subunit L.

In all calculations, we consider an RP with a single ^{13}C-spin and evaluate the total polarization generated through singlet-state and triplet-state recombination, P_S and P_T, respectively. To keep the DR contribution we evaluate the total CIDNP using eq. (7). Here we use $\xi = 0.98$ so that CIDNP comes predominantly from anisotropic mechanisms and take $k_S = 0.015$ ns^{-1} and $k_T = 0.4$ ns^{-1}. For the electron-electron coupling we assume that $d = -2J - D \approx -2J < 0$ (hence J-coupling is dominating over dipolar coupling). In the HFC tensor, we consider only the secular term $a = A_{zz}$ and the pseudo-secular term $b = \sqrt{A_{zx}^2 + A_{zy}^2}$ (the expression for the b-term is valid because the mutual orientation between the electron-electron and the electron-nuclear interaction tensors is not important in the present case). We run calculations of the CIDNP field dependence for specific orientations and also consider polarization averaged over all possible orientations. To describe rotations of the molecular system we introduce two angles, $0 < \theta < \pi$ and $0 < \varphi < 2\pi$. To introduce the components of the spin interaction tensors in the lab frame, we perform Euler rotations of the tensors in the molecular frame by using the rotation angles $\{\alpha, \beta, \gamma\} = \{\varphi, \theta, 0\}$ (the third rotation is not necessary due to the axial symmetry of the lab frame). One should note that there are different ways of defining Euler rotations, even in magnetic resonance literature. Here we rotate first about the z-axis, then about the new y'-axis, and finally about the new z''-axis

(this is the convention used, e.g., in Ref. 28). As a result, for different orientations we have different values of Δg_{zz}, a and b (electronic dipolar coupling is assumed to be small). In the calculation we use parameters of the nucleus **C13Φ** (acceptor) and make calculations for all possible orientations of the reaction center with respect to the $\mathbf{B}_0$ field, keeping the relative orientations of the spin interaction tensors unchanged. The hyperfine tensor was computed by density functional theory[27] starting from the coordinate frame of PDB structure 1AIJ[29], where the active bacteriopheophytin corresponds to residue 285 in chain L. In the molecular frame of the optimized structure, the unit vector along the porphyrin plane normal, defined by the normalized cross product of nitrogen-nitrogen vectors N_A-N_C and N_B-N_D, has the coordinates (0.2230, 0.7974, 0.5608).

We want to emphasize that in the present case the triplet RP state is relatively short-lived. Consequently, since the k_T value is 0.4 ns^{-1}, the lifetime broadening of the triplet states is about 400 MHz, which is significantly larger than the HFC terms. Nonetheless, the spin dynamics in RPs provides the selectivity to the nuclear spin state, which is required to generate CIDNP. This is possible because the RP start from the longer-lived singlet state; interestingly, in this case fast decay of the triplet state can slow down interconversion and increase the total RP lifetime [17, 30, 31]. Thus, the required selectivity of the reaction yield is achieved and CIDNP is formed. One should also note that here, because of the relatively large k_S and k_T, we obtain rather moderate CIDNP values of the order of 1% or less.

III. Results and discussion

We first analyze the results for specific orientations and then discuss the orientation and field dependence. Below we present examples corresponding to different orientations of RC. Some orientations can be analyzed in a relatively simple way using the LC/LAC concept; some of them are more difficult to interpret because of the complex spin dynamics and contributions from several mechanisms.

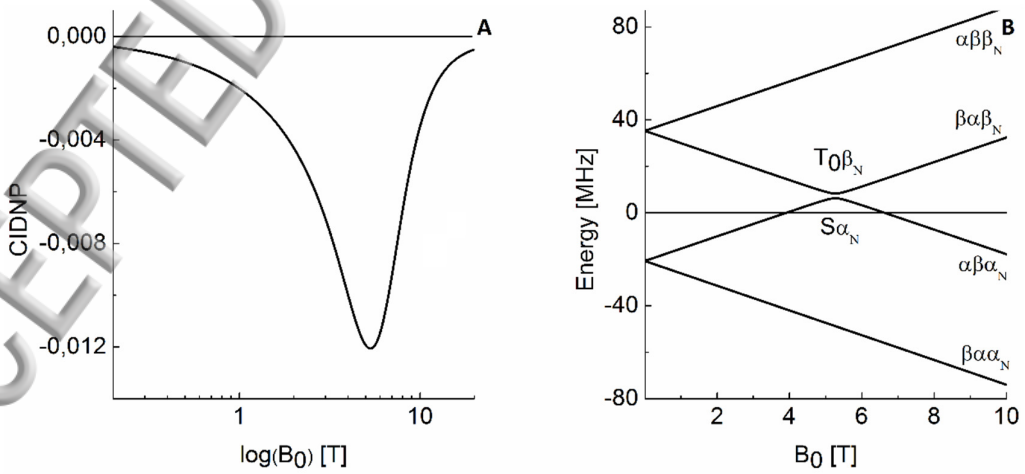

Figure 4. (A) CIDNP field dependence in example 1 and (B) scheme of RP energy levels. Simulation parameters: $g_A = g_D = 2.0031$, nucleus is a ^{13}C nucleus, $a = -0.05$ mT, $d = -2$ mT, $b = 0.15$ mT; $k_S = 0.015$ ns^{-1}, $k_T = 0.4$ ns^{-1}, $\xi = 0.98$. Emissive maximum in the CIDNP field dependence corresponds to the LAC between the states $S\alpha_N$ and $T_0\beta_N$.

This manuscript was accepted by J. Chem. Phys. Click here to see the version of record.

Example 1: orientation where $\Delta\omega_e = 0$, $a = -0.05$ mT, $d = -2$ mT. The four eigen-states of the RP (in the S-T_0 manifold of states) away from the LAC region are $T_0\alpha_N$, $S\alpha_N$, $T_0\beta_N$, $S\beta_N$ (at the LAC point), see **Figure 4**. The emissive minimum in the field dependence is the effect of the LAC between the states $S\alpha$ and $T_0\beta$; the matching field is $B_{LC} = \frac{\sqrt{d^2+\frac{a^2}{4}}}{\gamma_N}$. The sign rule is the one valid for the TSM case, see eq. (14). This case has been described in detail in our previous publication.[12]

Example 2: orientation where $|\Delta\omega_e| \approx |\omega_N|$, $a = -0.04$ mT, $d = -1.53$ mT

The four energy levels are (from bottom to top): $\beta\alpha\alpha_N$, $\beta\alpha\beta_N$, $\alpha\beta\alpha_N$, $\alpha\beta\beta_N$ (as specified at the highest magnetic field in **Figure 5**). In this case, DD, TSM and DR mechanisms contribute to the total polarization. In this situation, the TSM and DD mechanisms dominate. Since for both mechanisms CIDNP is negative, the resulting polarization is also negative. Indeed, for TSM the sign rule (14) gives $\Gamma = -1$; for DD, we also obtain $\Gamma = -1$ from the rule (13) (here $\epsilon = -1$, because $k_S < k_T$). The sign of polarization caused by DR, i.e., by the isotropic mechanism, is given by the rule (12), predicting $\Gamma = +1$ (here $\psi = 1$, because $\xi < 1$ and the singlet recombination channel dominates). The total polarization is negative as the TSM mechanism dominates over other contributions.

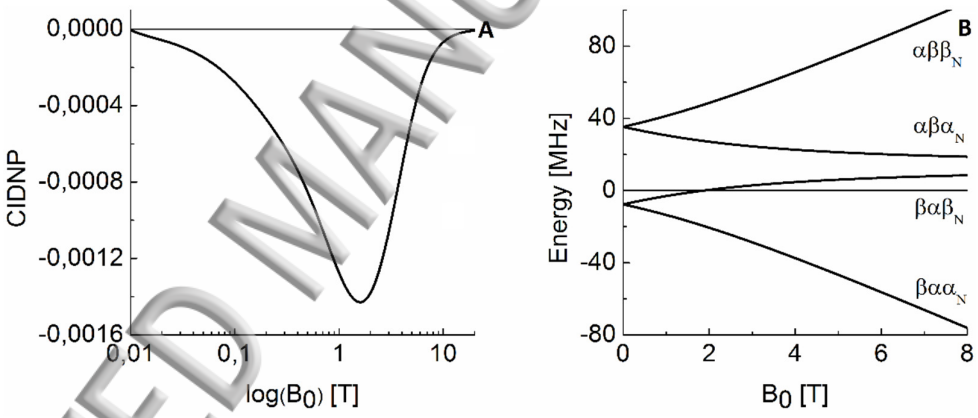

Figure 5. (A) CIDNP field dependence in example 2 and (B) scheme of RP energy levels. Simulation parameters: $g_A = 2.0034, g_D = 2.0027$, nucleus is a ^{13}C nucleus, $a = -0.04$ mT, $d = -1.53$ mT, $b = 0.15$ mT; $k_S = 0.015$ ns^{-1}, $k_T = 0.4$ ns^{-1}, $\xi = 0.98$. Emissive polarization is conditioned by the TSM and DD mechanisms.

For the sake of generality, we also considered a case, which is intermediate between examples 1 and 2; in this case $0 \neq |\Delta\omega_e| < |\omega_N|$. This case is considered in detail in **Supplementary Materials**.

Example 3: orientation where $|\Delta\omega_e| > |\omega_N|$, $a = -0.03$ mT, $d = -1.63$ mT

In this case, the polarization has two maxima, one of them is emissive, while the other one is absorptive, see **Figure 6**. At a first glance, the field dependence can be explained by the new mechanism reported here. However, a more thorough analysis (presented in **Supplementary Materials**) shows that in reality polarization comes from several contributions. Specifically, the DR-mechanism predicts positive polarization, the new mechanism predicts two maxima (emissive maximum at a lower field and absorptive maximum at a higher field), the DD mechanism predicts

This manuscript was accepted by J. Chem. Phys. Click here to see the version of record.

a negative maximum. Due to superposition of these mechanisms, a bimodal field dependence of CIDNP is observed.

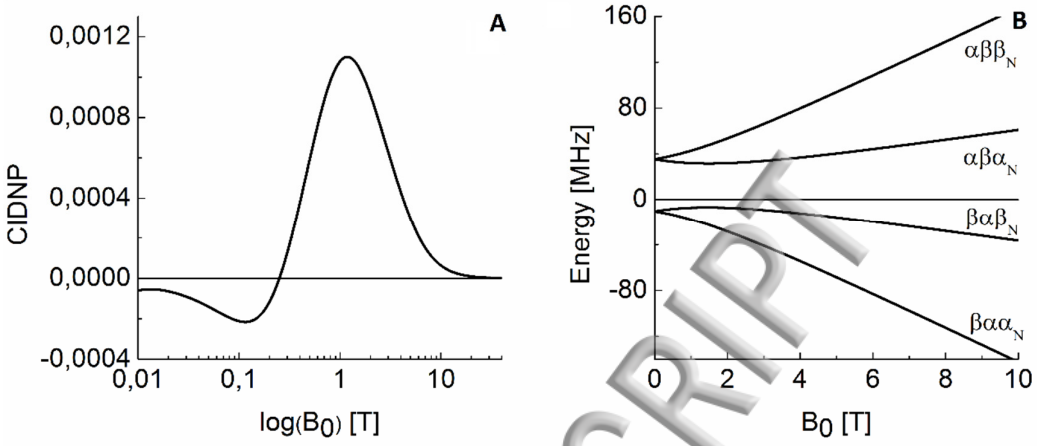

Figure 6. (A) CIDNP field dependence in example 3 and (B) scheme of RP energy levels. Simulation parameters: $g_A = 2.0035, g_D = 2.0021$, nucleus is a ^{13}C nucleus, $a = -0.03$ mT, $d = -1.63$ mT, $b = 0.17$ mT; $k_S = 0.015\text{ns}^{-1}, k_T = 0.4\text{ns}^{-1}, \xi = 0.98$.

Example 4. A more detailed analysis shows that the CIDNP field dependence can exhibit an even more complex behavior. In general, the field dependence of polarization depends not only on the relation between $|\Delta\omega_e|$ and $|\omega_N|$, but also on the HFC parameters (its secular part a and pseudo-secular part b), d-value and reaction rates. To demonstrate this, we considered one more example taking the following parameters:$|\Delta\omega_e| > |\omega_N|$, $a = -0.11$mT, $d = -1.63$mT.

Formally, these conditions correspond to those where the new mechanism becomes manifest. Indeed, this mechanism contributes to polarization formation. On the other hand, the field dependence is not exactly the same as that expected for the new mechanism, see **Figure 7**, since the positive maximum has additional structure. This additional feature originates from isotropic spin mixing, i.e., DR-mechanism or DD-mechanism. A more detailed analysis of the sign rules (not presented here) allows us to reject isotropic spin mixing. Hence, it is the DD-mechanism, which is responsible for the additional structure. Therefore, in general, total polarization is produced by a combination of several mechanisms.

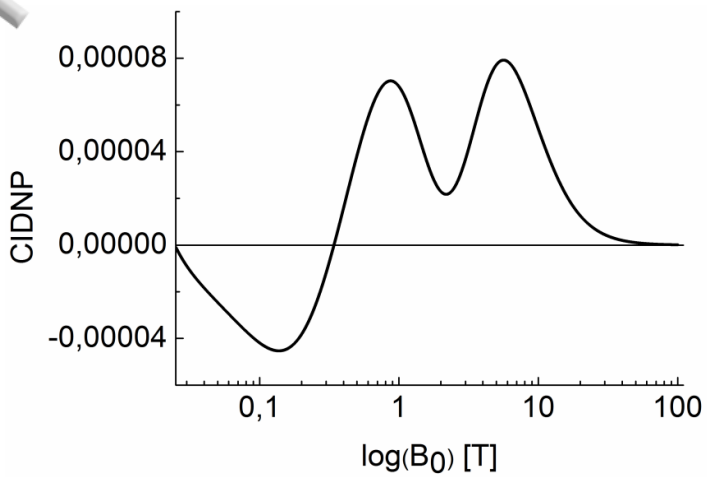

Figure 7. CIDNP field dependence in example 4. Simulation parameters: $g_A = 2.0023, g_D = 2.0032$, nucleus is a ^{13}C, $a = -0.11$ mT, $d = -1.63$ mT, $b = 0.11$ mT; $k_S = 0.015$ ns^{-1}, $k_T = 0.4$ ns^{-1}, $\xi = 0.98$.

This manuscript was accepted by J. Chem. Phys. Click here to see the version of record.

CIDNP averaged over orientations. Consideration of CIDNP for specific orientations allows us to rationalize the positions of features in the field dependence of polarization and the role of different interactions in polarization formation. Having analyzed CIDNP for specific orientations, we can now calculate and interpret the field dependence averaged over all orientations. The orientations are specified by setting two angles, θ and φ, which define orientation of the molecular frame with respect to the lab frame. Generally, three Euler angles are required to perform frame rotation; however, we keep in mind that in the lab frame there is axial symmetry (the symmetry axis is given by the external field direction).

The CIDNP field dependence averaged over all possible orientations has a positive and a negative maximum, see **Figure 8**, at the magnetic field of 0.4 T and 5 T, respectively. The amplitude of the positive feature is approximately 70 times lower than the amplitude of the negative feature; this result is in a qualitative agreement with the experimental field dependence for the **C13Φ** nucleus, see **Figure 1**, when we set $\xi = 0.977$. Such a field dependence is the result of interplay of (1) positive polarization that can be attributed to the DD and DR mechanisms; and (2) negative polarization originating from the TSM mechanism with the maximum of polarization given by the matching condition $|\omega_N| \approx |d|$. For demonstration that such interpretation is valid, we performed calculations of the angular dependence of CIDNP at specific field strengths, which correspond to the positive and negative maxima. In addition, we correlate the angular dependence of CIDNP with the angular dependence of different spin interactions.

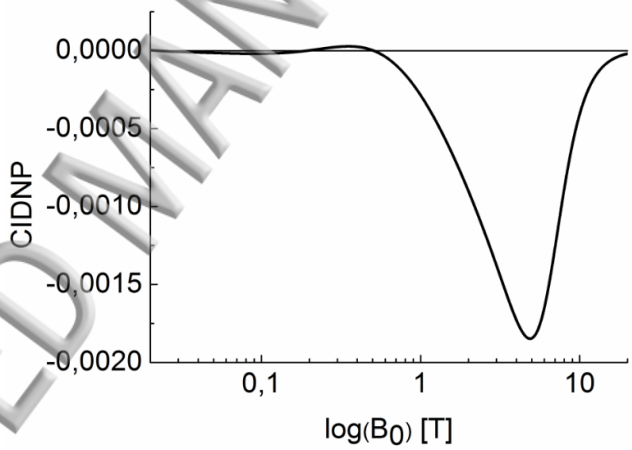

Figure 8. CIDNP field dependence of a photosynthetic reaction center protein of *Rhodobacter sphaeroides* averaged over all possible orientations. Simulation parameters: nucleus is the ^{13}C nucleus **C13Φ**; $k_S = 0.015$ ns^{-1}, $k_T = 0.4$ ns^{-1}, $\xi = 0.98$.

By rotating the sample, one changes different components of the spin interaction tensors, which affect the spin dynamics. To gain insight into polarization formation, we correlate the orientation dependence of CIDNP with the orientation dependence of specific tensor components and reveal the role of different mechanisms in polarization formation. For instance, at high magnetic field of 5 T (see the orientation dependence of polarization shown in **Figure 9**) we conclude that the TSM-mechanism is dominating giving rise to negative CIDNP. We can draw this conclusion from the fact that TSM works best when $|\Delta\omega_e|$ is small, i.e., when $|\Delta g|$ tends to zero. The orientation dependence of $|\Delta g|$ is presented in **Figure 10**: indeed, the regions where Δg is small (dark blue regions) correlate with those where CIDNP is strong (dark blue regions in **Figure 9**). For CIDNP formation, it is also necessary that the pseudo-secular HFC term is non-zero; for this reason, we

This manuscript was accepted by J. Chem. Phys. Click here to see the version of record.

also plotted the angular dependence of the b-term. When the angular dependences (contour maps shown in **Figures 10** and **11**) of Δg and b are superimposed the orientation dependence of CIDNP (shown in **Figure 9**) is well reproduced.

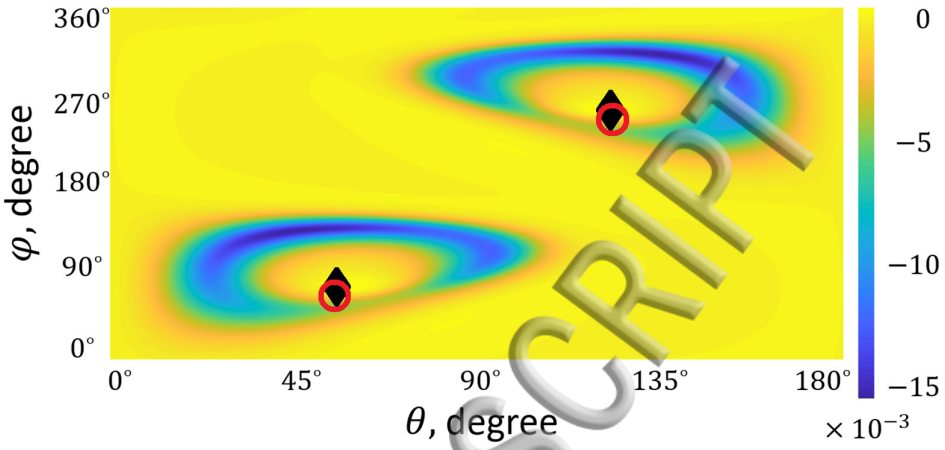

Figure 9. Angular dependence of CIDNP at the 5 T field strength, corresponding to the negative maximum in the field dependence. There are two regions in this contour plot where strong CIDNP (blue) is expected. The plane normal of the bacteriopheophytin is marked by full diamonds ($\theta = 55.9°$, $\varphi = 74.4°$ and symmetry equivalent) and the principal axis of the ^{13}C hyperfine tensor corresponding to the largest principal value of 30.8 MHz is marked by open circles ($\theta = 55.1°$, $\varphi = 64.8°$ and symmetry equivalent).

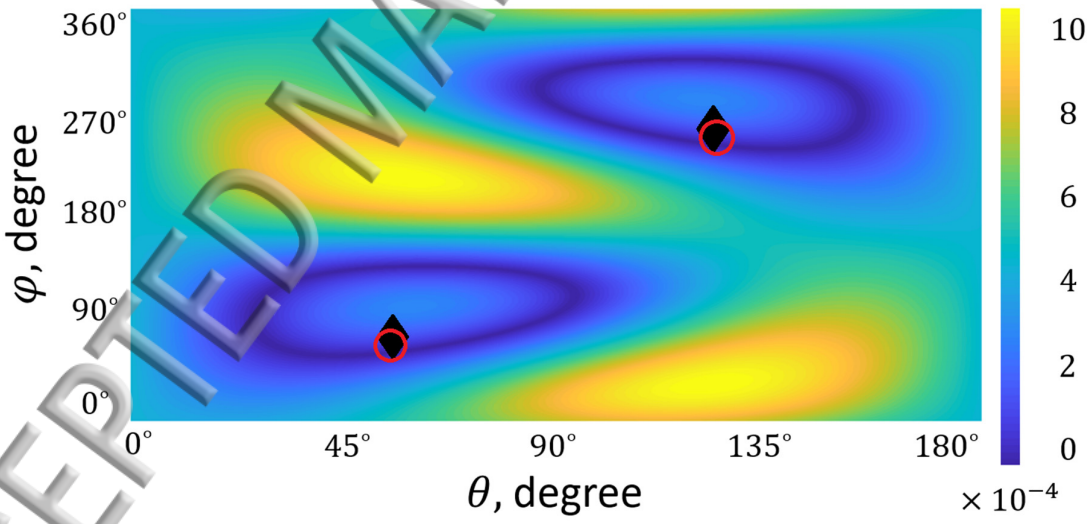

Figure 10. Angular dependence of $|\Delta g|/g_e$ (here g_e is the g-factor of the free electron). The plane normal of the bacteriopheophytin is marked by full diamonds and the principal axis of the ^{13}C hyperfine tensor corresponding to the largest principal value is marked by open circles.

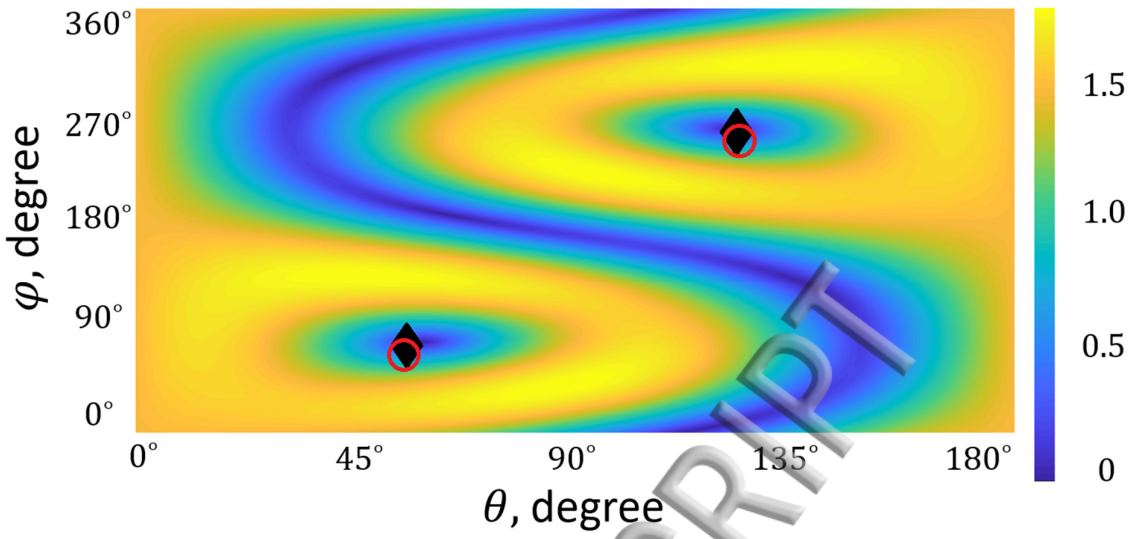

Figure 11. Angular dependence of the *b* term (pseudo-secular HFC). The plane normal of the bacteriopheophytin is marked by full diamonds and the principal axis of the ^{13}C hyperfine tensor corresponding to the largest principal value is marked by open circles.

The angular dependence of polarization at low fields is more difficult to analyze because different mechanisms provide contributions to CIDNP of comparable amplitude. The orientation dependence of CIDNP at 0.1 T is shown in **Figure 12**. One can see that at different orientations polarization can be positive as well as negative because different mechanisms dominate at different orientations. Altogether, the orientations giving positive CIDNP are dominant and the resulting polarization is positive. Hence, polarization comes from interplay of at least two mechanisms, DD and DR.

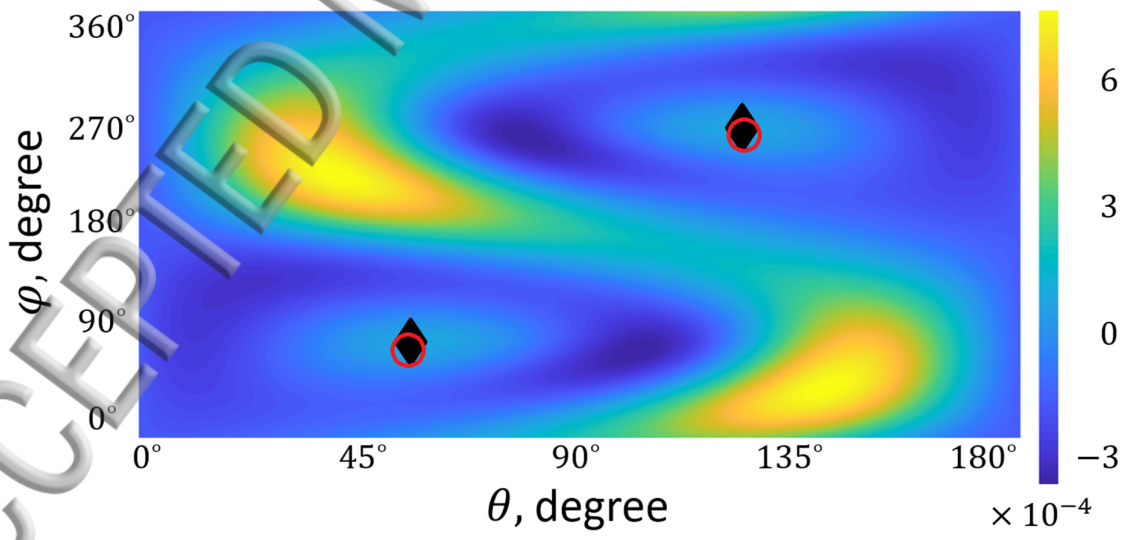

Figure 12. Angular dependence of CIDNP at the 0.1 T field strength, corresponding to the negative maximum in the field dependence. There are two regions in this contour plot where CIDNP is strong and positive and also regions where it is strong and negative. The plane normal of the bacteriopheophytin is marked by full diamonds and the principal axis of the ^{13}C hyperfine tensor corresponding to the largest principal value is marked by open circles.

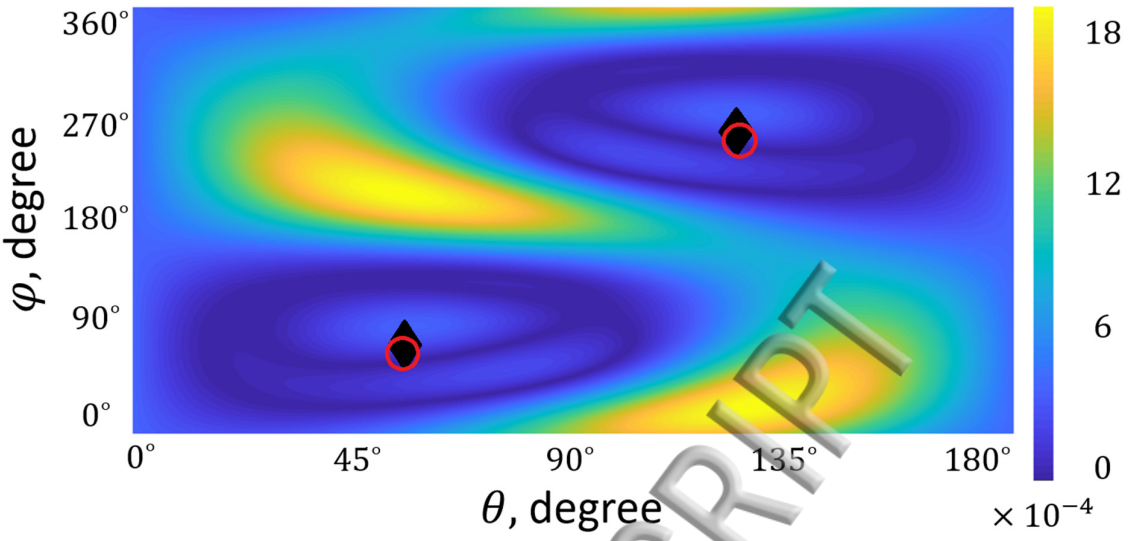

Figure 13. Angular dependence of $|a \cdot \Delta g|/g_e$ (here g_e is the g-factor of the free electron). The plane normal of the bacteriopheophytin is marked by full diamonds and the principal axis of the ^{13}C hyperfine tensor corresponding to the largest principal value is marked by open circles.

According to the sign rules of polarization caused by DD and DR, CIDNP is determined mostly by the Δg and a terms in the spin Hamiltonian. For this reason, we also show the contour plot for the product $|\Delta g \cdot a|$, see **Figure 13**. Red and blue regions reflect the correlation between CIDNP and $|\Delta g \cdot a|$ value. One can clearly see that this contour plot correlates with the angular dependence of CIDNP shown **in Figure 12**. This allows us to conclude that at low fields polarization is determined mostly by the DD and DR mechanisms, whereas at high field polarization formation is conditioned by the TSM mechanism.

IV. Conclusions

Theoretical analysis of the CIDNP field dependence in photosynthetic reaction centers performed here allows us to obtain good qualitative agreement with the experimentally measured field dependences. Detailed consideration of the field dependence at different orientations allows us to conclude that at different orientations different CINDP mechanisms are dominant, which give rise to features in the B_0 dependences emerging at different fields. In fact, features in the CIDNP field dependence are conditioned by polarization formed at specific orientations. We have analyzed the angular dependence of CIDNP at low and high fields and compared it to the angular dependence of different anisotropic interactions. Correlation between the orientation dependence of CIDNP and spin interactions allows us to obtain dominant contributions to polarization. At high fields, the main contribution to polarization comes from the TSM mechanism, so the position of the high-field feature can be deduced from the condition $|\omega_N| \approx |d|$. At low fields, a more complex behavior is obtained, which comes from the DD and DR mechanisms. Hence, different mechanisms become pronounced in different magnetic field ranges. For this reason, the field dependence and orientation dependence of polarization need to be analyzed together in order to explain the experimental findings.

In this context, it is worthwhile to discuss solution of the inverse problem, that is the determination of the RP parameters from the CIDNP field dependence. Solution of such a problem is generally complex and ambiguous. The ambiguity, however, can be reduced by additional information about

the system – e.g. by knowing the reaction scheme (such information can be obtained from independent optical or EPR experiments), by knowing the molecular geometry (in the case of photosynthetic reaction centers such information can be taken from X-ray data) – such information can significantly restrict the parameter space. In addition, CIDNP data can be obtained for a set of magnetic nuclei, e.g. ^{1}H, ^{13}C and ^{15}N. Such measures can be extremely helpful to (i) identify the dominant CIDNP mechanism (or mechanisms) and (ii) to obtain RP parameters by fitting the experimental field dependences. In the present case, some of the parameters of the system are known; likewise, the reaction scheme has been determined independently. This knowledge allows us to identify the key role of the TSM-mechanism and to estimate the d value (and its sign) from the high-field feature in the field-dependence. A similar situation holds in the case of liquid-state CIDNP, where the values of J_{ex}, a and Δg can be extracted by fitting the experimental B_0-dependences of polarization using a suitable theoretical model. We expect that the strategy for analyzing the CIDNP field dependence in other cases is similar even despite the more complex spin dynamics.

The situation considered here does not present the most complex case of CIDNP formation. The reason is that the exchange coupling dominates over the dipolar coupling. For this reason, we can always assume that d does not depend strongly on the orientation and its sign is always the same. For dipolar coupling, one should consider the orientation dependence of the d-term and its sign change. Since the sign of CIDNP depends on the sign of d, we expect that the orientation dependence of polarization becomes even more complex; likewise, the field dependence of CIDNP is expected to exhibit additional features. Ideally, analysis of CIDNP in such cases should be performed in single crystals, which is possible in some cases.[2-4,32, 33] Such a study is, however, beyond the scope of the present work.

Acknowledgements

This work was supported by the Russian Science Foundation (grant No. 15-13-20035). J.M. would like to acknowledge the Deutsche Forschungsgemeinschaft for generous support (MA 4972/11-1).

References

[1] K. M. Salikhov, Y. N. Molin, R. Z. Sagdeev, and A. L. Buchachenko, *Spin polarization and magnetic effects in chemical reactions* (Elsevier, Amsterdam, 1984),

[2] H. Schuch, D. Stehlik, and K. H. Hausser, Z. Naturforsch. **26a** (1971) 1944.

[3] D. Stehlik, in *Excited States*, edited by E. C. Lim (Academic Press, New York, 1977).

[4] G. Buntkowsky, M. Nack, D. Stehlik, and H.-M. Vieth, Isr. J. Chem. **29** (1989) 109.

[5] B. E. Bode, S. S. Thamarath, K. B. Sai Sankar Gupta, A. Alia, G. Jeschke, and J. Matysik, Top. Curr. Chem. **338** (2013) 105.

[6] A. McDermott, M. G. Zysmilich, and T. Polenova, Solid State Nucl. Magn. Reson. **11** (1998) 21.

[7] T. Polenova, and A. E. McDermott, J. Phys. Chem. B **103** (1999) 535.

[8] I. C. Camacho, and J. Matysik, in *The Biophysics of Photosynthesis*, edited by J. G. A. v. d. Est (Springer, 2014), pp. 141.

[9] A. Diller, E. Roy, P. Gast, H. J. van Gorkom, H. J. M. de Groot, C. Glaubitz, G. Jeschke, J. Matysik, and A. Alia, Proc. Natl. Acad. Sci. U. S. A. **104** (2007) 12767.

[10] S. S. Thamarath, B. E. Bode, S. Prakash, K. B. S. S. Gupta, A. Alia, G. Jeschke, and J. Matysik, J. Am. Chem. Soc. **134** (2012) 5921.

[11] S. S. Thamarath, J. Heberle, P. J. Hore, T. Kottke, and J. Matysik, J. Am. Chem. Soc. **132** (2010) 15542.

[12] D. V. Sosnovsky, G. Jeschke, J. Matysik, H.-M. Vieth, and K. L. Ivanov, J. Chem. Phys. **144** (2016) 144202.

[13] D. Gräsing, P. Bielytskyi, I. F. Céspedes-Camacho, A. Alia, T. Marquardsen, F. Engelke, and J. Matysik, Sci. Rep. **7** (2017)

[14] M. Wegner, H. Fischer, S. Grosse, H.-M. Vieth, A. M. Oliver, and M. N. Paddon-Row, Chem. Phys. **264** (2001) 341.

[15] G. Lindblad, Commun. Math. Phys. **48** (1976) 119.

[16] R. Haberkorn, Mol. Phys. **32** (1976) 1491.

[17] K. L. Ivanov, M. V. Petrova, N. N. Lukzen, and K. Maeda, J. Phys. Chem. A **114** (2010) 9447.

[18] J. Jones, and P. J. Hore, Chem. Phys. Lett. **488** (2010) 90.

[19] G. Jeschke, J. Chem. Phys. **106** (1997) 10072.

[20] G. Jeschke, J. Am. Chem. Soc. **120** (1998) 4425.

[21] G. Jeschke, and J. Matysik, Chem. Phys. **294** (2003) 239.

[22] U. Till, I. B. Klenina, I. I. Proskuryakov, A. J. Hoff, and P. J. Hore, J. Phys. Chem. B **101** (1997) 10939.

[23] R. J. Hulsebosch, I. V. Borovykh, S. V. Paschenko, P. Gast, and A. J. Hoff, J. Phys. Chem. B **103** (1999) 6815.

[24] R. J. Hulsebosch, I. V. Borovykh, S. V. Paschenko, P. Gast, and A. J. Hoff, J. Phys. Chem. B **105** (2001) 10146.

[25] R. Klette, J. T. Törring, M. Plato, K. Möbius, B. Bönigk, and W. Lubitz, J. Phys. Chem. **97** (1993) 2015.

[26] P. Dorlet, A. W. Rutherford, and S. Un, Biochem. **39** (2000) 7826.

[27] S. Prakash, P. Gast, H. J. M. de Groot, G. Jeschke, and J. Matysik, J. Am. Chem. Soc. **127** (2005) 14290.

[28] M. Mehring, *Principles of High-Resolution NMR in Solids* (Springer Verlag, Berlin-Heidelberg-New York, 1983),

[29] M. H. Stowell, T. M. McPhillips, D. C. Rees, S. M. Soltis, E. Abresch, and G. Feher, Science **276** (1997) 812.

[30] I. V. Koptyug, N. N. Lukzen, E. G. Bagryanskaya, and A. B. Doktorov, Chem. Phys. Lett. **175** (1990) 467.

[31] V. L. Berdinskii, and I. N. Yakunin, Dokl. Phys. Chem. **421** (2008) 163.

[32] G. Dittrich, D. Stehlik, and K. H. Hausser, Z. Naturforsch. **A32** (1977) 652.

[33] D. Stehlik, P. Rösch, P. Lau, H. Zimmermann, and K. H. Hausser, Chem. Phys. **21** (1977) 301.

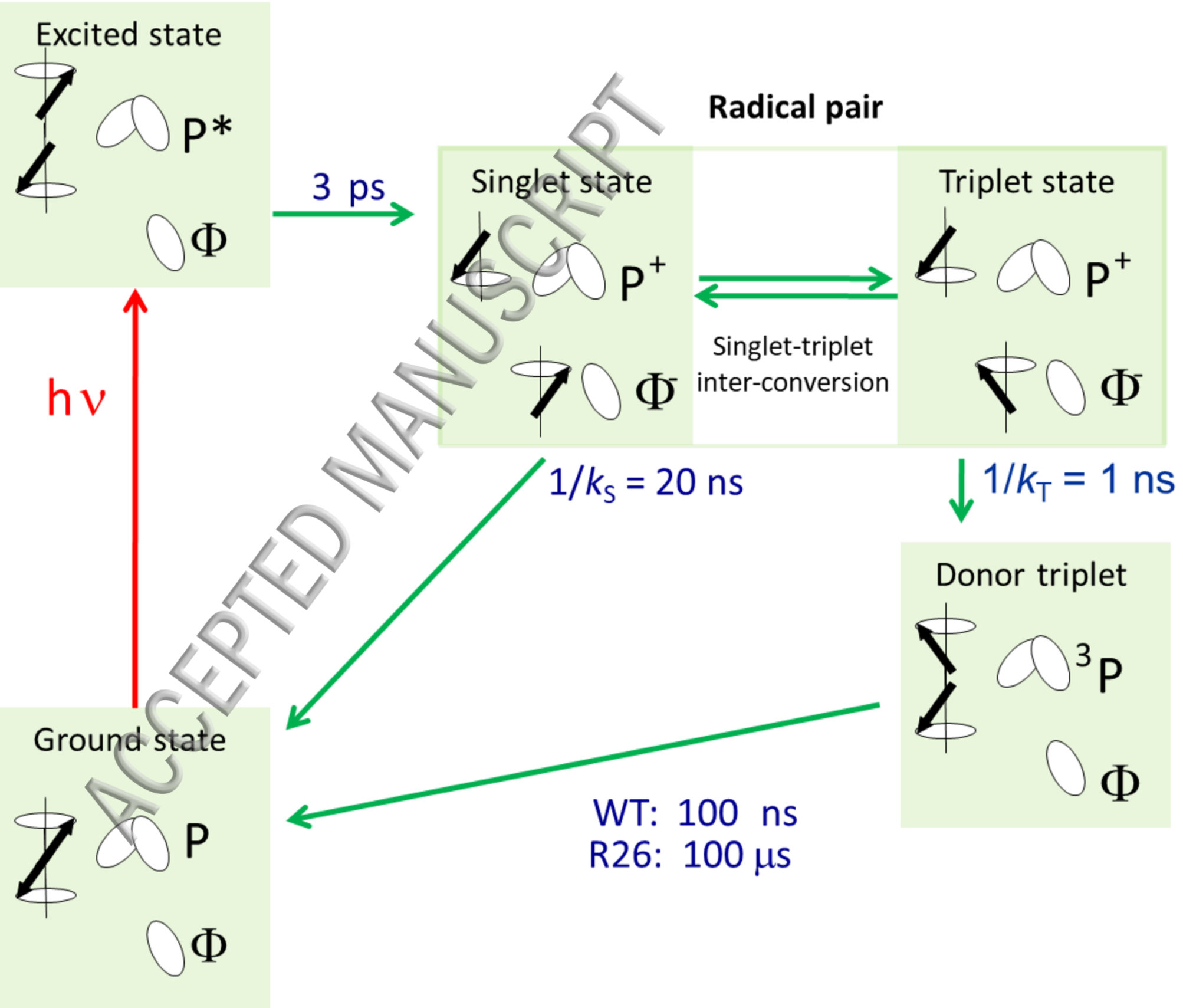

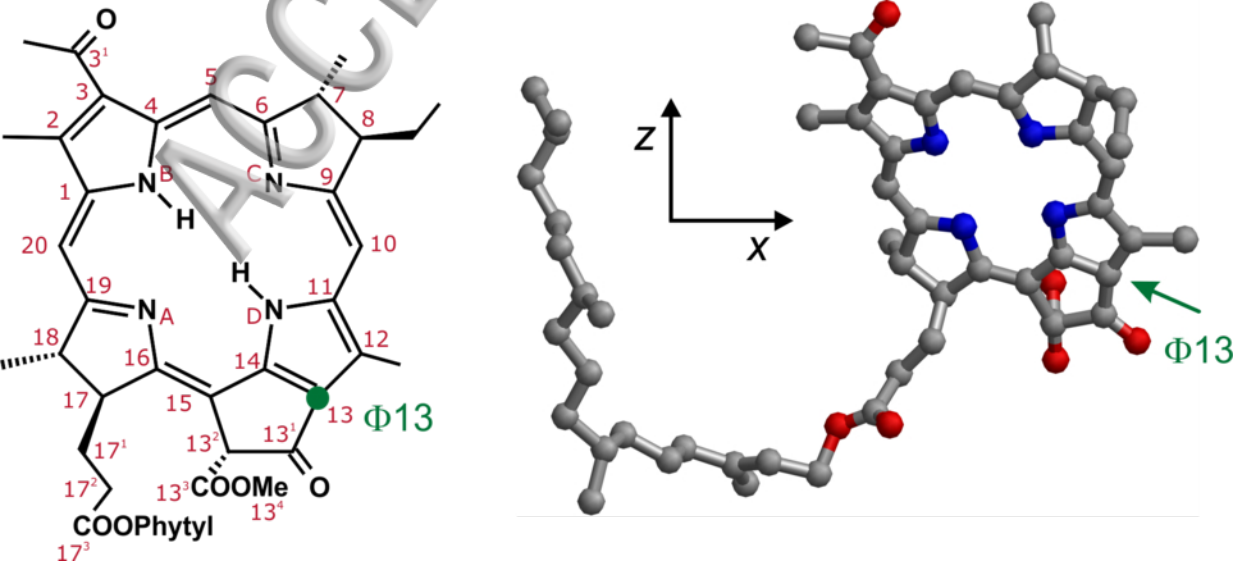
O
3¹
3
4
5
6
7
8
2
1
N B
H
C N
9
20
10
19
N A
H
D N
11
18
16
14
12
17
15
13
Φ13
17¹
13²
13¹
17²
13³COOMe
O
13⁴
COOPhytyl
17³
Z
X
Φ13

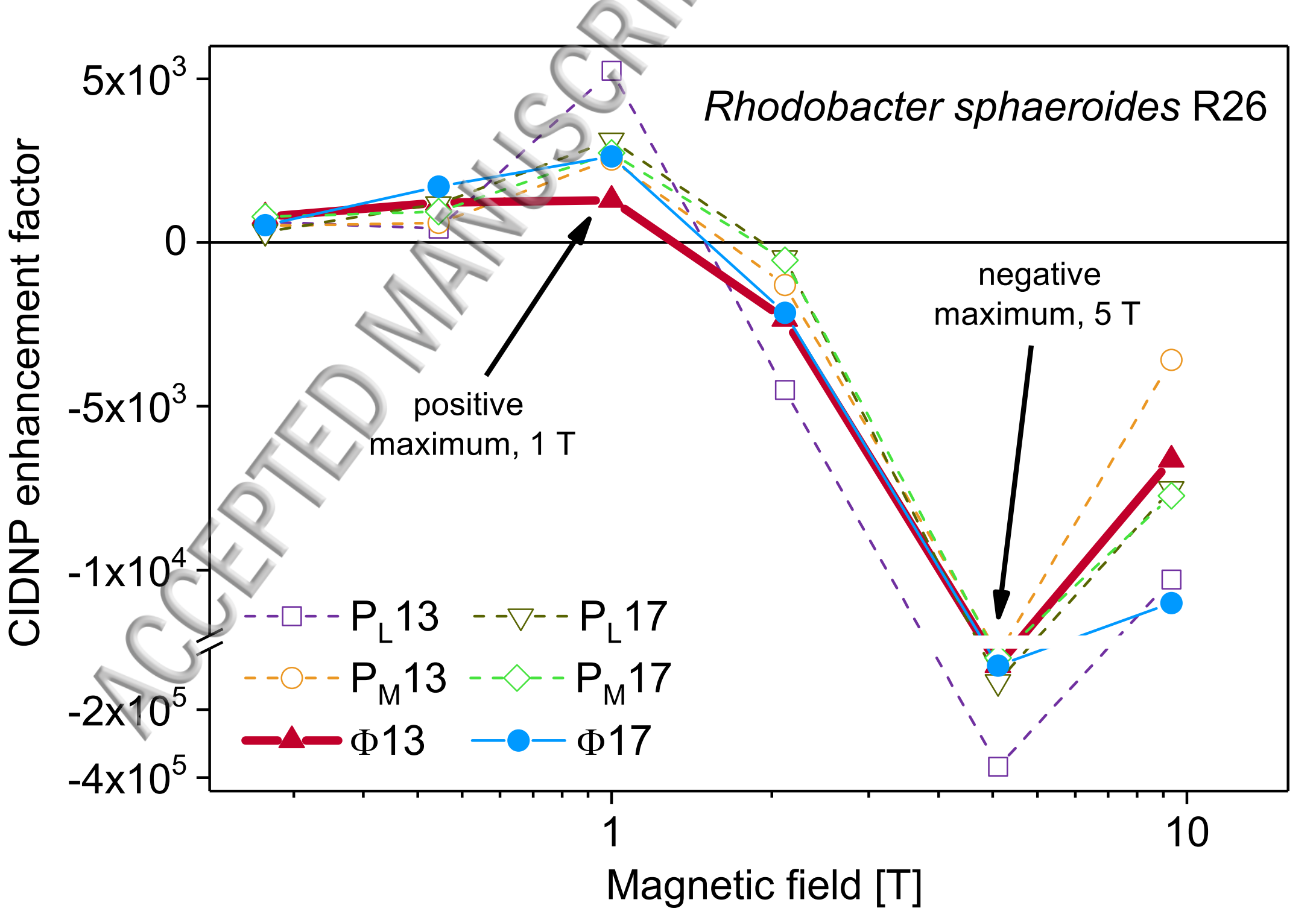

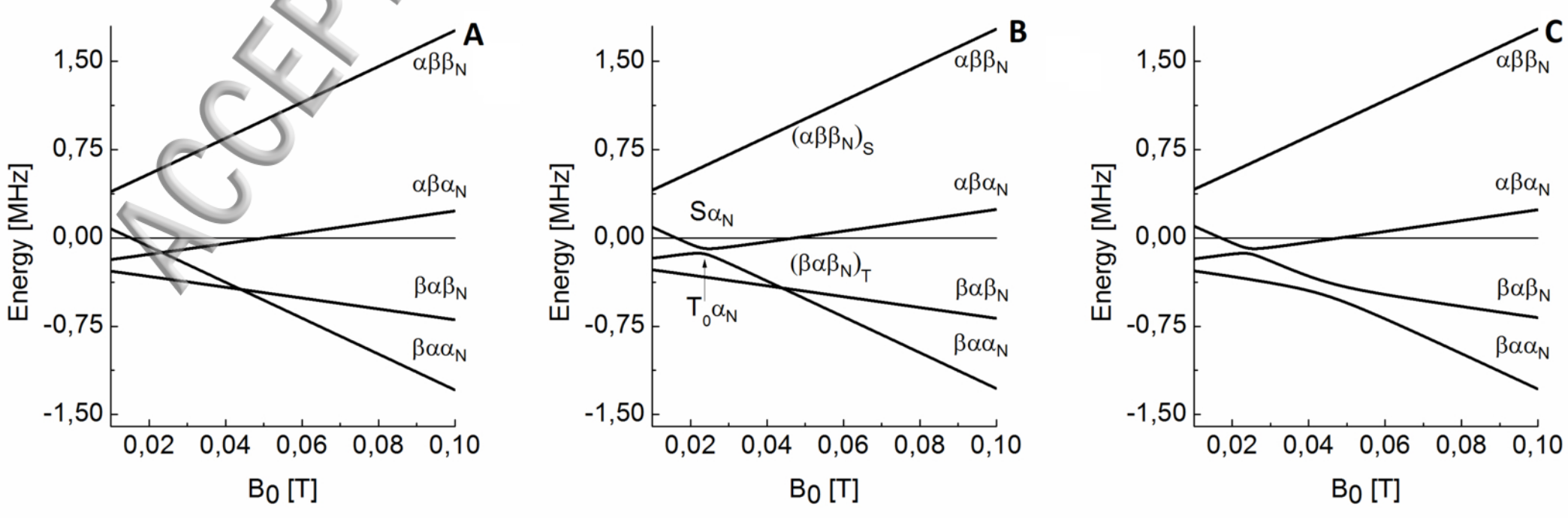
A
B
C
1,50
0,75
0,00
-0,75
-1,50
Energy [MHz]
0,02
0,04
0,06
0,08
0,10
B0 [T]
αββN
αβαN
βαβN
ββαN
(αββN)S
SαN
(βαβN)T
T0αN